BIOCHIMICA ET BIOPHYSICA ACTA
BBA

Permeation of phloretin across bilayer lipid membranes monitored by dipole potential and microelectrode measurements

Peter Pohl *, Tatyana I. Rokitskaya [1], Elena E. Pohl, Sapar M. Saparov

Martin-Luther-Universität, Medizinische Fakultät, Institut für Medizinische Physik und Biophysik, 06097 Halle, Germany

Received 13 June 1996; revised 5 September 1996; accepted 11 September 1996

Abstract

The transmembrane diffusion of phloretin across planar bilayer lipid membranes is studied under steady-state conditions. Diffusion restrictions and adsorption related effects are measured independently. The adsorption of aligned phloretin dipoles generates a change in the intrinsic dipole potential difference between the inner and outer leaflets of the lipid bilayer. It is monitored by capacitive current measurements carried out with a direct current (dc) bias. The variation of the intramembrane electric field indicates a saturation of the binding sites at the membrane interface. In contrast, pH profile measurements undertaken in the immediate membrane vicinity show a constant membrane permeability. If phloretin binding and transmembrane diffusion are treated as two competitive events rather than subsequent steps in the transport queue the contradictory results become explainable. A mathematical model is developed where it is assumed that diffusing phloretin molecules are randomly oriented, i.e., that they do not contribute to the intrinsic membrane potential. Only the dipoles adsorbing onto the membrane are oriented. Based on these theory the membrane permeability is calculated from the capacitive current data. It is found to agree very well with the permeability deduced from the microelectrode measurements.

Keywords: Unstirred layer; Bilayer lipid; Phloretin; Dipole potential; Diffusion; Microelectrode

1. Introduction

Phloretin and phloretin-like electrolytes strongly modify the permeability of biological membranes. An increase of the cation [1] and a decrease of the anion conductance [2] of the membrane are found. These changes are contributed to a decrease of the positive dipole potential of the membrane due to phloretin orienting in the membrane [3]. In addition phloretin inhibits chloride [4], urea [5] and hexose [6] transporters. Again changes in the dipole potential seem to be responsible. It is suggested that the anomalous selectivity and conductivity of some potassium channels can be explained by the existence of a dipolar potential source near the mouth of the channel [7]. Furthermore the ion flux induced by the nonelectrogenic ionophores nigericin and tributyltin is altered by phloretin [8].

Distinct structural changes are observed for the phosphocholine head group after the adsorption of

* Corresponding author. Fax: +49 345 5571632; E-mail: peter.pohl@medizin.uni-halle.de

[1] Permanent address: A.N. Belozersky Institute of Physico-Chemical Biology, Moscow State University, Moscow 119899, Russia.

PII S0005-2736(96)00185-X

phloretin to the membrane [9]. Phloretin also modifies the hydration layer at the lipid/water interface [9], that makes a major contribution to the dipole potential of the membrane [10]. The relationship between the phloretin induced change in the dipole potential and the aqueous concentration of the molecule is well described by a Langmuir isotherm [11]. Although the binding of phloretin to a lipid membrane is a saturable process, the permeation kinetics appear to be unsaturable. To explain the surprising behaviour the presence of multiple types of binding sites is suggested by Verkman and Solomon [12]. In contrast to red blood cells, where one binding site is related to membrane proteins and the other to lipids, the existence of a second binding site is not shown yet for protein free membranes.

In the present paper, the unsaturable transmembrane transport kinetics of phloretin is explained differently. Lipid binding to a single class of sites is treated as an event competitive to transmembrane movement rather than being an obligate step in the transport queue. Microelectrode measurements of concentration profiles within the unstirred layers (USLs) [8] combined with recordings of the dipole potential difference between the two layers of a membrane [13] permit to determine the membrane permeability in a wide phloretin concentration range. Both methods are chosen because they do not disturb the system under investigation, especially they do not require modifications of the membrane. In the presence of a steady-state periodic membrane potential the properties of transmembrane diffusion of a neutral molecule are measured. This work seeks to show that useful new information can be obtained by means of capacity current measurements undertaken with a dc bias even for the case of adsorption and diffusion of uncharged molecules. Restrictions to the investigation of dipole modificators adsorbing in their charged form are overcome [14]. The method requires only steady-state measurements – similar to the approach proposed by Horn [15] for measuring the dynamic properties of nonelectrogenic transporters. In contrast to the measurement of frequency response functions of nonelectrogenic [15] or electrogenic transporters [16] the current is monitored at one single frequency. Changes in the intrinsic dipole potential of bilayer lipid membranes (BLM) are used to monitor transport kinetics. The theoretical model developed is confirmed by measurements of proton concentration changes detected in the immediate membrane vicinity.

2. Theory

The interaction between membranes and phloretin can be monitored by spectrophotometric [17], fluorescence quenching [18] techniques, dual-wavelength ratiometric fluorescence measurements of the membrane dipole potential [19] or using NMR [9]. On model membranes a variety of electrical methods is exploited, all of them based on the fact that phloretin dramatically increases cation and decreases anion conductances of membranes treated with ion carriers [1,11,20]. The accuracy of the investigations can be enhanced by measuring the binding and translocation rates of hydrophobic cation and anion spin labels in unilamellar vesicle systems formed from phosphatidylcholine [3].

An approach for following the transmembrane movement of phloretin is proposed by Jennings and Solomon [21]. A rapid pH rise detected in an unbuffered cell suspension represents the uptake of the undissociated form of the weak acid phloretin (T). Chemical reactions ($T^- + H^+ \rightleftharpoons TH$) are responsible for the depletion of H^+ in the extracellular medium. However the presence of buffer can increase the rate of weak acid absorption [22]. A detailed analysis of weak acid transport across planar lipid bilayers in the presence of buffers is carried out with the help of pH microelectrodes. The experimentally proven model takes into account multiple proton-transfer reactions occurring in the USLs adjacent to the membrane [23]. The particular system reported (acetate as the weak acid and Tris and Mes as the buffer mixture) is very similar to the one studied in the present paper. The fluxes of the protonated (TH) and deprotonated (T^-) forms of phloretin as well as the fluxes of the other solutes are described by Fick's law of diffusion:

$$J_i = -D_i \mathrm{d}c_i/\mathrm{d}x,\ i = 1,\ldots,8 \quad (1)$$

The mass balance is given by:

$$\mathrm{d}J_i/\mathrm{d}x = R_i(c),\ i = 1,\ldots,8;\ c = (c_1,\ldots,c_8) \quad (2)$$

Here, J_i, D_i, $c_i(x)$, are, respectively, the flux, the diffusion coefficient and the concentration of the *i*-th

species, where $1 = H^+$, $2 = T^-$, $3 = TH$, $4 = OH^-$, $5 = A^{2-}$, $6 = AH^-$, $7 = B$, $8 = BH^+$ (A and B are buffer molecules). $R_i(c)$ is the specific local rate of expenditure of the i-th species in the chemical reactions:

$$H^+ + T^- \underset{k_{+1}}{\overset{k_{-1}}{\rightleftharpoons}} TH;\ H^+ + OH^- \underset{k_{+2}}{\overset{k_{-2}}{\rightleftharpoons}} H_2O$$

$$H^+ + Mes^{2-} \underset{k_{+3}}{\overset{k_{-3}}{\rightleftharpoons}} MesH^-;\ H^+ + Tris \underset{k_{+4}}{\overset{k_{-4}}{\rightleftharpoons}} TrisH^+ \quad (3)$$

At the membrane/water interface, the fluxes of all species are required to be equal to zero except for J_3, so that

$$J_1 = J_2 = J_4 ... = J_8 = 0;\ J_3 = P^M\left([TH]_1^M - [TH]_2^M\right) \quad (4)$$

where P^M is the membrane permeability and $[TH]_1^M$ and $[TH]_2^M$ are, respectively, the local concentrations of the neutral form of phloretin at the first and the second surface of the membrane. The numerical solution is derived assuming that the rates of chemical reactions (like dissociation/recombination of water, buffers and phloretin) are very high compared to the rate of diffusion through the USL, so that the local chemical equilibrium is maintained. Other boundary conditions are formulated in [23]. There are only three unknown parameters in this system: the membrane permeability of phloretin and the kinetic constants $k_{\pm 1}$. Since the pK value for phloretin is known to be 7.3 [21] only two independent parameters are left to be determined by the numerical algorithm.

Another approach to determine the membrane permeability of phloretin becomes available from the knowledge of the amount of phloretin bound to the outer and inner leaflets of the membrane. The orienting of the phloretin dipoles in the membrane accompanied by an imparting of a dipole potential of opposite polarity to the preexisting one is described by the following reaction [17]:

$$TH^M + L \underset{k_{+5}}{\overset{k_{-5}}{\rightleftharpoons}} TH^A$$

where TH^A is the adsorbed acid, TH^M the uncharged free acid in the near of the membrane/water interface and L the free lipid binding place. The adsorption of phloretin is accompanied with a dipole potential change φ. φ becomes available from conductance measurements performed on BLM doped with nonactin [24]:

$$G/G_0 = \exp[\, zF\varphi/RT\,] \quad (5)$$

where G and G_0 denote the conductance in the presence and absence of the dipolar adsorbate respectively. R, T and F have their usual meanings. In this case the phloretin concentrations at both sides of the membrane are equal and the concentration in the bulk does not differ from the one in the immediate membrane vicinity. Using this approach DeLevie et al. [24] and Reyes et al. [11] have shown that the relationship between the change in the dipole potential φ and the aqueous concentration of phloretin is well described by a Langmuir isotherm. The change in the existing space-averaged dipole potential is proportional to the concentration of the molecules adsorbed [11]:

$$\frac{[TH]^M}{K_d} = \frac{[TH]^A}{N - [TH]^A} = \frac{\varphi}{\varphi^{max} - \varphi} \quad (6)$$

where the apparent dissociation constant K_d is equal to k_{+5}/k_{-5}. N denotes the total concentration of binding places ($N = [L] + [TH]^A$). φ and φ^{max} are the dipole and the maximal dipole potential changes.

Under the conditions of a transmembrane phloretin concentration gradient conductance measurements do not give exact information about the contributions of each monolayer to the total dipole potential change. It can be obtained without any modifications of the membrane measuring the second harmonic of the capacitive current. The overtone is generated by the intramembrane asymmetry of the dipole potential. The absolute value of the difference between the dipole potentials of the two monolayers $\Delta\varphi$ is equal to the bias of the ac-current where the second harmonic component vanishes (see e.g., Ref. [13]). Consequently the intramembrane field compensation method can be used to monitor the kinetics of phloretin adsorption and transmembrane movement and the effective transmembrane translocation rate ν^m can be found. Taking into account lipid binding, phloretin dissociation and diffusion across the USLs (with ν^{ul} as the transport rate across the USL) the changes of the interfacial concentrations of the free

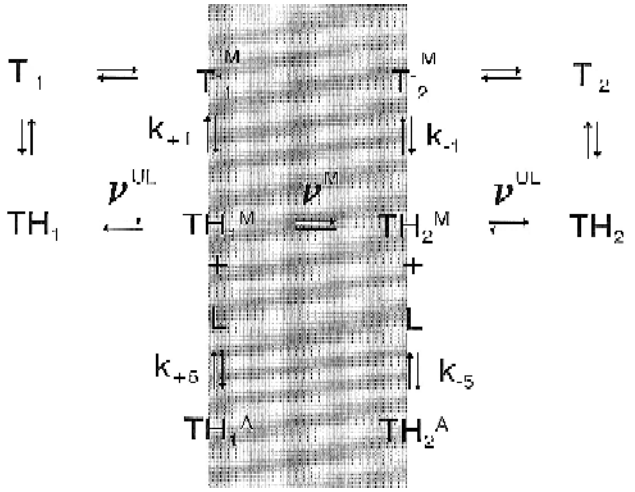

Fig. 1. Both the protonated (TH) and deprotonated (T^-) forms of phloretin are able to diffuse across the unstirred layer to the membrane surface where their concentrations $[TH]^M$ and $[T^-]^M$ differ from those in the bulk. Here, the subscripts 1 and 2 designate the different sides of the membrane. TH^A denotes phloretin molecules bound to the lipid (L). The binding reaction is treated as an event competitive to transbilayer movement rather than being a step in the transport queue. The forward and backward reaction rates of proton (k_{+1}, k_{-1}) and lipid binding (k_{+5}, k_{-5}) are assumed to be several orders of magnitude higher than the rate of diffusion across the unstirred layer (ν^{UL}) and the membrane (ν^M).

and bound phloretin with time are given by the following six differential equations (see Fig. 1):

$$\frac{d[TH]_1^M}{dt} = \nu^{ul}[TH]_1 - \nu^{ul}[TH]_1^M - k_{-5}[TH]_1^M\left(N - [TH]_1^A\right) + k_{+5}[TH]_1^A - \nu^m\left([TH]_1^M - [TH]_2^M\right) + k_{-1}[H^+][T^-]_1^M - k_{+1}[TH]_1^M \quad (7)$$

$$\frac{d[TH]_2^M}{dt} = -\nu^{ul}[TH]_2^M - k_{-5}[TH]_2^M\left(N - [TH]_2^A\right) + k_{+5}[TH]_2^A + \nu^m\left([TH]_1^M - [TH]_2^M\right) + k_{-1}[H^+][T^-]_2^M - k_{+1}[TH]_2^M \quad (8)$$

$$\frac{d[TH]_1^A}{dt} = k_{-5}[TH]_1^M\left(N - [TH]_1^A\right) - k_{+5}[TH]_1^A \quad (9)$$

$$\frac{d[TH]_2^A}{dt} = k_{-5}[TH]_2^M\left(N - [TH]_2^A\right) - k_{+5}[TH]_2^A \quad (10)$$

$$\frac{d[T^-]_1^M}{dt} = \nu^{ul}[T^-]_1 - \nu^{ul}[T^-]_1^M - k_{-1}[H^+][T^-]_1^M + k_{+1}[TH]_1^M \quad (11)$$

$$\frac{d[T^-]_2^M}{dt} = k_{+1}[TH]_2^M - \nu^{ul}[T^-]_2^M - k_{-1}[H^+][T^-]_2^M \quad (12)$$

It is reasonable to assume the same transport rate across the USL for both T^- and TH because the diffusion coefficient in water is related to the molecular weight that is nearly the same for both substances. Furthermore it is assumed that phloretin is added only to compartment 1 and that, with respect to the large bulk volume, the concentrations $[TH]_2$ and $[T^-]_2$ in the second compartment are negligible small. The differential Eqs. (6)–(12) may be reduced in the steady state to the following single expression for the measured intramembrane dipole potential drop $\Delta\varphi$:

$$\frac{\Delta\varphi}{\varphi^{max}} = \frac{[TH]_1^A - [TH]_2^A}{N} = \frac{[T_0](1 + a + \alpha)}{K_d(1 + \alpha)(1 + 2a + \alpha) + [T_0](1 + a + \alpha)} - \frac{[T_0]a}{K_d(1 + \alpha)(1 + 2a + \alpha) + [T_0]a} \quad (13)$$

with the notation: $a = \nu^m/\nu^{ul}$, and $\alpha = [T^-]/[TH] = 10^{pH - pK}$. $[T_0]$ is the total concentration of phloretin added to side 1.

3. Materials and methods

3.1. Membrane formation

The BLMs were formed by a conventional method [25] in a hole, 0.8 mm in diameter, of a diaphragm of a PTFE chamber. The membrane forming solution contained 20 mg diphytanoyl phosphatidylcholine

(Avanti Polar Lipids, Alabaster, AL) dissolved in 1 ml of n-decane (Merck, Darmstadt, Germany). A solution consisting of 1 mM Tris (Fluka, Buchs, Switzerland), 1 mM Mes (Boehringer, Mannheim, Germany), 1 mM CAPSO (Sigma, St. Louis, MO) and 100 mM KCl (Fluka, Buchs, Switzerland) surrounded the bilayers. It was agitated by magnetic bars.

Alcoholic solutions of phloretin (Fluka) were added at one side of the membrane.

3.2. Monitoring of the dipole potential drop between the lipid layers using the Inner Field Compensation (IFC) method

The intrinsic membrane potential can be measured by capacitance minimization [26]. The capacitive current of the membrane contains a signal harmonic to the fundamental frequency (418 Hz) applied which vanishes if a dc signal coinciding with the boundary potential difference is transferred to the reference electrodes additionally to the ac signal. Sokolov [13] was the first who used second harmonics to measure the potential difference between the boundaries of a BLM. The boundary potential of the membrane is originated from surface and dipole potentials. Since phloretin is assumed to affect the dipole potential only the IFC method gives the possibility to measure the dipole potential difference $\Delta\varphi$.

For monitoring $\Delta\varphi$ a sine wave input voltage (source: Model 33120A, Hewlett–Packard, Loveland, CO) was applied to the membrane. The output signal was first amplified by a current amplifier (Model 428, Keihley Instruments, Cleveland, OH) and than filtered to reduce the amplitude of the signal with the fundamental frequency. The second harmonic was detected by a lock-in amplifier (HMS Elektronik, Leverkusen, Germany). Due to the connection of both the generator and the lock-in amplifier to an IEEE interface of a personal computer the dc offset required to minimize the amplitude of the overtone was automatically calculated and applied to the membrane. The adjustment and the storage of the offset were performed every second.

3.3. Microelectrode measurements

The transmembrane flux of a weak acid generates a concentration gradient of protons within the USL [22]. This gradient was measured in terms of the potential difference between a pH microelectrode and a reference electrode as described earlier [27]. The voltage data were recorded by an electrometer (Model 617, Keihley Instruments, Cleveland, OH) and transferred via an IEEE-interface to a personal computer.

The pH sensors were made of glass capillaries containing antimony. After pulling their tips they had a diameter of about 5–10 μm. The pH electrodes were moved by a hydraulic microdrive manipulator (Narishige, Tokyo, Japan). The touching of the membrane was indicated by a steep change of pH electrode potential [8]. Since the velocity of the electrode motion was known (2 μm s^{-1}) the position of the pH sensor relatively to the membrane could be determined at any instant of the experiment. The accuracy of the distance measurements was limited by the lack of a definite reference position for the membrane surface. It was assumed to be situated between the onset of the steep potential change and the breakdown of the BLM. The former was used as reference quantity. Usually the withdrawal of the electrode started before the membrane was ruptured. A maximum total error of ± 8 μm was estimated.

3.4. Conductance measurements

Current–voltage relationships were measured by the current amplifier (Model 428, Keihley Instruments, Cleveland, OH) using the built-in voltage source. The effect of phloretin on the nonactin-induced conductance was used to study its adsorption behaviour at different pH values [2]. The change in the dipole potential φ was deduced from the relation of the initial conductance G_0 and the conductance G in the presence of phloretin (Eq. (5)).

4. Results

The binding of phloretin to a planar bilayer membrane is monitored in terms of dipole potential changes φ. φ is calculated from the conductance of a BLM doped with nonactin (Eq. (5)). The latter is measured as a function of both the phloretin concentration and the pH value of the medium. A bell like shape is found for the dependence of φ from the pH

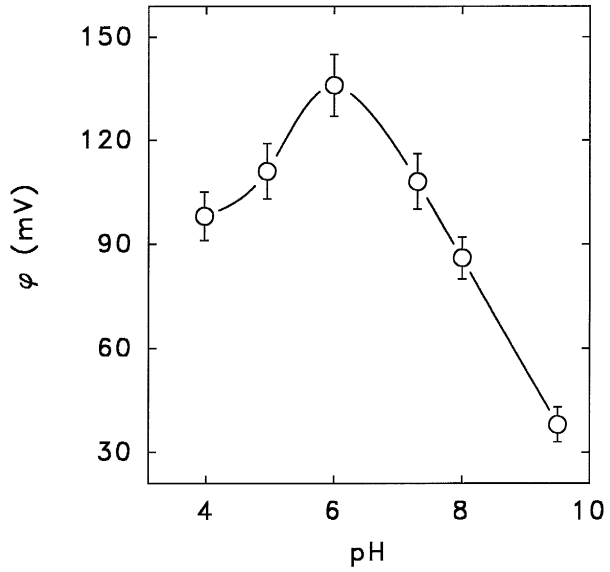

Fig. 2. pH dependence of the dipole potential changes φ at a constant phloretin bulk concentration. φ is calculated from conductance measurements of a BLM doped with nonactin. The solution contained 50 μM phloretin, 0.1 μM nonactin, 20 mM Tris, 20 mM Mes, 20 mM CAPSO, 100 mM KCl.

bulk value. For one particular phloretin bulk concentration $[T_0]$ it is shown in Fig. 2. Since only the uncharged form of phloretin (TH) adsorbs to the membrane φ is expected to decrease with an increase in pH ($pH > pK$). The declining effect of phloretin on the dipole potential at $pH < 6$ can be attributed to a loss of affinity to the binding sites. From the concentration dependence of φ it is possible to obtain K_d and φ^{max}. After a linear transformation (φ is plotted versus $\varphi/[TH]^M$) the constants are acquired as the slope and the intercept of the regression line [11]. This transformation is consistent with the Langmuir adsorption isotherm given by Eq. (6) [11]. Whereas φ^{max} is nearly invariant with pH (190 ± 10 mV) K_d depends on the pH value of the medium (data not shown). Over the pH range 4 to 10 it can be well approximated by the polynomial:

$$K_d = 77 - 14\,pH + 0.642\,pH^2 \qquad (14)$$

In a low buffered medium the diffusion of phloretin along a concentration gradient through a BLM causes a pH shift in the USL. Fig. 3 demonstrates examples of pH profiles recorded in the USL of a BLM at pH 7, obtained after a 20-fold reduction of the buffer concentration compared with Fig. 2.

From an uniexponential fitting of the pH profile the USL thickness at one side of the membrane is found to be 200 ± 15 μm (compare [27]):

$$pH(x) = (pH^M - pH^{bulk})e^{-x/\delta} + pH^{bulk} \qquad (15)$$

where pH^{bulk} and pH^M are the pH values in the bulk and in the immediate membrane vicinity, respectively.

The difference between the pH values in the bulk and in the immediate membrane vicinity ΔpH appears to be a function of the phloretin concentration in the bulk (Fig. 3). The mathematical model derived from the Eqs. (1)–(4) is used to calculate the membrane permeability [23]. Assuming a diffusion coefficient D of $5.5 \cdot 10^{-6}$ cm^2 s^{-1} for phloretin [20] a value of $2.4 \cdot 10^{-4}$ cm/s is obtained. The agreement between the theoretical predicted and experimental measured ΔpH is good at low phloretin concentrations (see Fig. 5). The deviations between theory and experiment occurring at higher concentrations can be contributed to the inconsistency of the generally accepted model of the 'unstirred layer' assuming the existence of a strict boundary between the regions of 'pure diffusion' and 'ideal stirring' [23].

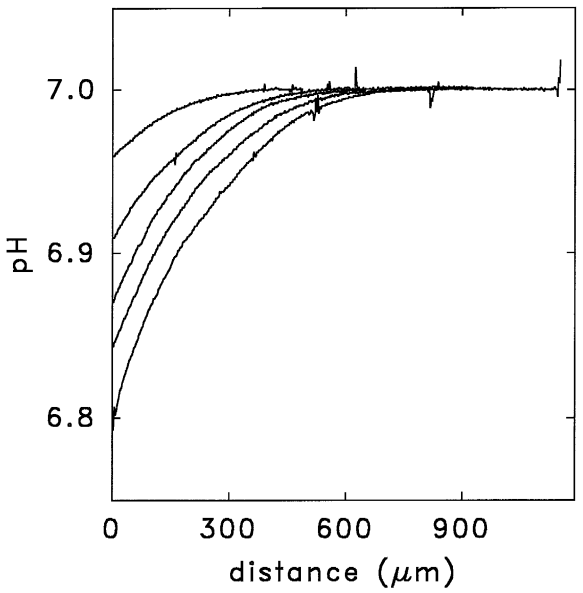

Fig. 3. Examples of pH profiles in the immediate membrane vicinity (trans side) induced by the permeation of phloretin. The solution contained 1 mM Tris, 1 mM Mes, 1 mM CAPSO, 100 mM KCl. pH was 7. In steps of 0.2 mM the phloretin concentration at the cis side was increased from 0.2 mM (upper curve) to 1 mM.

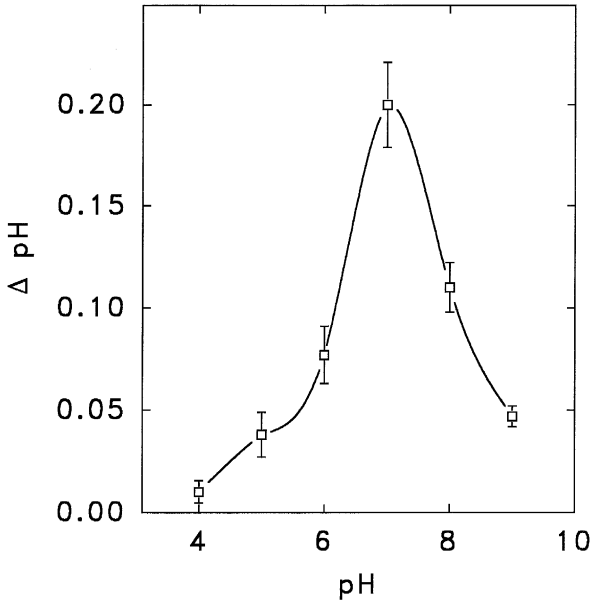

Fig. 4. pH shift in the immediate membrane vicinity as a function of the pH value of the bulk. The cis buffer solution (see Fig. 3) contained 1 mM phloretin.

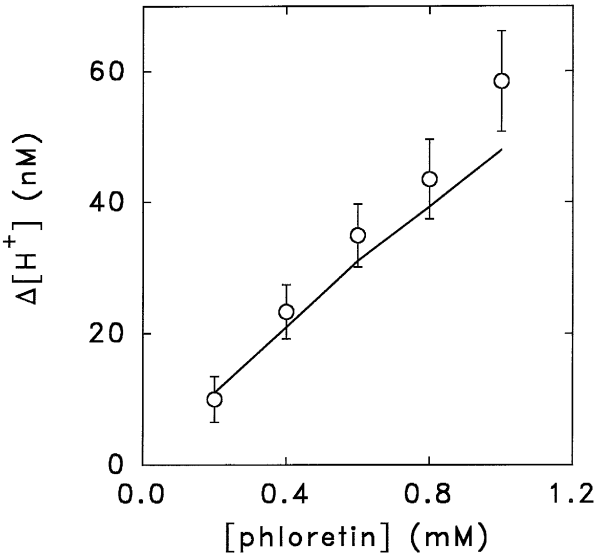

Fig. 5. Proton concentration shifts at the trans membrane/water interface obtained from pH profiles. Conditions as in Fig. 3. The spline line was calculated from the knowledge of the diffusion coefficients and the pK values of phloretin and the buffer (Tris, Mes) molecules as published earlier [23].

The pH shift at the membrane/water interface induced by the permeation of a weak acid is expected to depend on the pH value of the bulk [28]. ΔpH has a maximum near the pK value of phloretin (Fig. 4). It decreases at high pH values (pH > pK) because the diffusion across the membrane itself becomes rate-limiting compared with the diffusion across the USLs [29]. At low pH values the concentration of the acid anion becomes negligible and so does the pH shift since it is produced by the dissociation of the proton from the transported acid [30].

Fig. 5 shows the proton concentration shifts at the trans membrane/water interface obtained from pH profiles as a function of the phloretin concentration.

The dipole potential difference between the membrane lipid layers is determined with the help of the inner membrane field compensation method. Both the concentration and the pH dependence can be modified by alterations of the USL thickness (Figs. 6 and 7). The effect of stirring, greatly pronounced at acidic pH values vanishes at basic ones. $\Delta\varphi$ has a bell like shape if plotted against the proton bulk concentration (Fig. 7), similar to ΔpH (Fig. 4). Remarkable is one difference – the invariance of $\Delta\varphi$ in the pH interval from 4 to 6 (Fig. 7). Unlike ΔpH that vanishes in

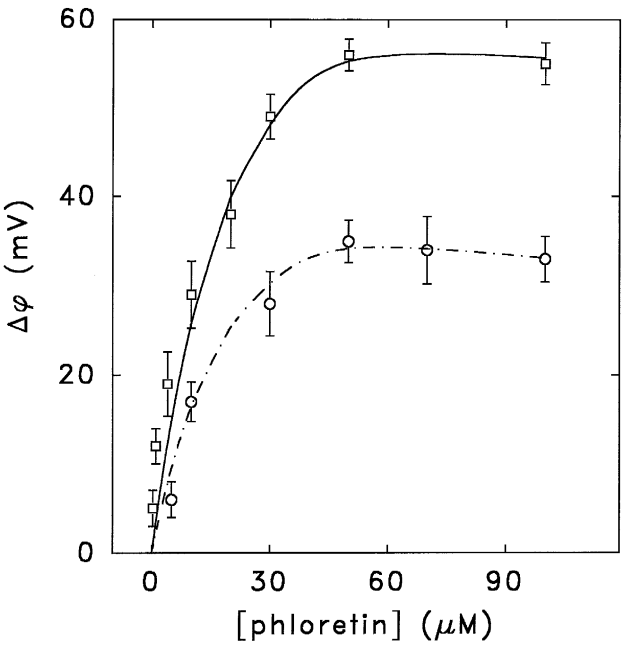

Fig. 6. The intramembrane dipole potential drop $\Delta\varphi$ as a function of the cis phloretin concentration at (as in the Figs. 3–5) a gentle (○) and a vigorous (□) stirring rate. The spline lines were calculated from Eq. (13). The ratios of the membrane and unstirred layer transport rates were set to 0.9 (lower trace) and 0.4 (upper curve), respectively.

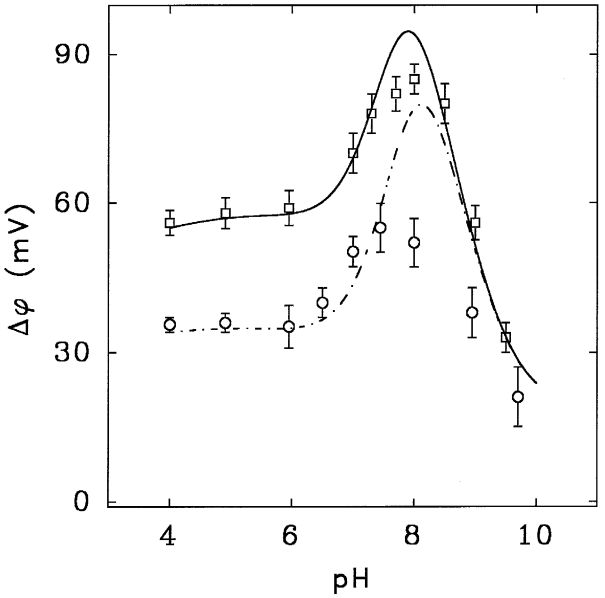

Fig. 7. Dependence of the intramembrane dipole potential drop $\Delta\varphi$ from the bulk pH at a phloretin concentration of 50 μM at the cis side. The spline lines were calculated from Eq. (13). The ratios of the membrane and unstirred layer transport rates were set to 0.9 for gentle stirring (○) and to 0.4 for vigorous stirring (□) conditions. The effective dissociation constant K_d appeared to be a function of pH and was determined via conductance measurements of membranes doped with nonactin.

parallel with the concentration of the acid anion $\Delta\varphi$ is related to the concentration of the protonated acid. From the peak value at pH 7 only a modest decrease of $\Delta\varphi$ is obtained in the acidic pH range. The conclusion may be drawn that neither the diffusion across the USL nor the diffusion across the membrane itself are rate-limiting, in other words the USL and the membrane permeabilities are of the same order of magnitude.

According to Eq. (13) the ratio of the rates of transmembrane movement and transport across the USL ν^M/ν^{UL} is found to be 0.9 ± 0.07 and 0.4 ± 0.05 for gently and rigorous stirring conditions (Figs. 6 and 7). Assuming that the thickness of the USL does not depend on the phloretin concentration gradient, i.e. that the USL permeability is invariant, the membrane permeability is calculated. A value of $(2.4 \pm 0.3) \cdot 10^{-4}$ cm/s is obtained.

The intramembrane dipole potential drop plotted as a function of the phloretin concentration shows a saturation-like behaviour (Fig. 6) that is predicted by the theory (Eq. (13)) with great accuracy.

5. Discussion

The rates of phloretin binding and release from the surface binding sites are extremely fast [17]. Even though binding of phloretin to a lipid membrane is a saturable process, the permeation kinetics appear to be unsaturable (Fig. 4). This result is in agreement with literature data [18,12]. A kinetic scheme is devised by Verkman and Solomon [12] to account for the observed linearity between the transmembrane equilibration rate and phloretin concentration by postulating two phloretin binding sites at each membrane interface. The translocation rate obtained is treated as the result of a combination of a rapid exchange of phloretin from a high-affinity membrane site to a low-affinity site. In fact the permeability coefficient would be a function of phloretin concentration, if the movement of phloretin between two interfacial binding sites is describable by a unimolecular rate process over a simple thermodynamic barrier. Because the translocation rate across the vesicular membrane does not deviate from linearity over the measured phloretin concentration range (0–50 μM) [12] the second binding site remains hypothetical. In the present study the phloretin concentration is increased more than 10-fold (up to 1 mM). Nevertheless the transmembrane flux is proportional to the phloretin bulk concentration within the whole concentration range (Fig. 5). Evidence for two binding sites is found in the case of erythrocytes but not in model systems. In the former case phloretin binds with high affinity ($K_d = 1.5$ μM) to membrane proteins and with low-affinity ($K_d = 54$ μM) to lipids [21]. Considering the linear dependence of the transport rate on the phloretin concentration one alternative explanation is that prior to phloretin permeation no adsorption at the interface is required. In other words virtually no bound phloretin diffuses across the membrane. Binding and transmembrane diffusion can be considered as two competitive events. Apparently, diffusing phloretin molecules are randomly oriented. This phloretin pool does not adopt a membrane orientation such that its

electric dipole moment counteracts the intrinsic membrane potential. It is therefore not detectable by means of dipole potential measurements. Only the adsorbed, i.e. oriented fraction of phloretin (TH^A) can be monitored this way. Even if the binding site should saturate for high phloretin concentrations ($\gg 30\ \mu M$) the membrane permeability coefficient remains independent of the phloretin bulk concentration.

If lipid binding is treated as an event competitive to transmembrane diffusion the latter becomes similar to the transmembrane movement of other weak acids and bases like salicylic acid [22], butyric acid [31] or acetic acid [23]. Qualitative agreement is found indeed. The pH shift in the USL plotted against bulk pH shows a bell like shape (Fig. 5) comparable to the one found for acetic acid and ammonium [30]. The membrane permeability coefficient of small nonelectrolytes does not depend on their concentration [32]. Moreover the dependence of ΔpH on the phloretin bulk concentration (Fig. 4) is predicted by a theoretical model of weak acid transport across BLMs in the presence of buffers [23].

The permeation of phloretin through a BLM is modeled in terms of discrete steps: diffusion through the USL of the charged and uncharged form, proton uptake of the anion at the water/membrane interface, binding to the membrane surface or alternatively translocation through the membrane, dissociation of phloretin or alternatively binding to the opposite membrane surface, and diffusion through the opposite USL (Fig. 1). The mathematical model (Eq. (13)) takes the pH dependence of phloretin binding into account. The steady-state binding constant K_d to a single class of high-affinity sites fitted by a polynomial (Eq. (14)) is in agreement with literature data ranging from $23 \pm 5\ \mu M$ [18] at pH 4.0 to $2.7 \pm 1.5\ \mu M$ at pH 9.3 [12]. The maximal value of the change in the existing space-averaged dipole potential of the DPhPC membrane (190 ± 10 mV) obtained is close to the values of 220 mV and 200 mV reported for phosphatidylethanolamine ([24] and [11], respectively) and to the value of 240 ± 20 mV calculated for egg phosphatidylcholine [33] membranes.

In Eq. (13) electrostatic interactions between the lipid bilayer and phloretin as well as dipole–dipole interactions are neglected. Because exclusively the uncharged form of phloretin adsorbs to the membrane [6,21] it is commonly accepted that the dipole potential is the only potential modified by the phloretin molecules [24]. This statement is supported by the fact that phloretin adsorbs to charged and uncharged membranes equally well [34] and by the observation that φ rapidly decreases at basic pH (Fig. 2). It is therefore most unlikely that lipid–phloretin interactions create changes of the small electrostatic surface potential (zeta-potentials in the order of several millivolts are measured) exhibited by pure phosphatidylcholine bilayers [35] which are able to affect further phloretin binding. Only the electric field originated by a bound phloretin dipole layer may probable alter K_d. But, both experimentally and theoretically, the dipole–dipole interaction is so weak that it has only a minor effect on the adsorption isotherm [24].

Modifications of the membrane's intrinsic dipole potential are linked to the diffusion rates through the USL and the membrane itself (Eq. (13)). Theoretical predicted and experimental measured changes in the dipole potential difference between the inner and outer membrane leaflets are in good agreement (Figs. 6 and 7). The most pronounced deviations are observed at neutral pH, where the transmembrane flux is maximal. It is well known that the transport rate of a weak acid is enhanced in the presence of buffers [22]. The resulting increase in the local concentrations $[TH]_2^M$ and $[TH]_2^A$ should be accompanied with a decrease of $\Delta\varphi$ as observed in the experiment. It is therefore most likely that the discrepancy between theory and experimental data set (Fig. 7) arises from the neglect of chemical reactions due to the presence of buffer molecules in the medium.

Two different approaches are used that are completely independent from each other: the intramembrane field compensation method and the microelectrode technique. As expected the ratio of the transport rates across the membrane (ν^M) and the USL (ν^{UL}) is equal to the ratio of the membrane (P^M) and USL layer permeabilities (P^{UL}) under the same gentle stirring conditions:

$$\frac{P^M}{P^{UL}} = \frac{\nu^M}{\nu^{UL}} = 0.9$$

Both methods give the same membrane permeability for phloretin. The value of $2.4 \cdot 10^{-4}$ cm s^{-1} coincides with the one reported for red cell membranes [21].

Acknowledgements

This work has been supported by the Kulturministerium des Landes Sachsen Anhalt, Germany (FKZ: 2218A/0085). One of the authors is indebted to the Deutscher Akademischer Austauschdienst (DAAD) for subsidizing his stay at the University Halle. The authors are grateful to Dr. Y.N. Antonenko (Moscow State University) and Dr. V.S. Sokolov (Frumkin Institute of Electrochemistry of the Russian Academy of Sciences, Moscow) for many helpful discussions.

References

[1] Andersen, O.S., Finkelstein, A. and Katz, I. (1976) J. Gen. Physiol. 67, 749–771
[2] Melnik, E., Latorre, R., Hall, J.E. and Tosteson, D.C. (1977) J. Gen. Physiol. 69, 243–257.
[3] Franklin, J.C. and Cafiso, D.S. (1993) Biophys. J. 65, 289–299.
[4] Cousin, J.L. and Motais, R. (1978) Biochim. Biophys. Acta 373, 151–164.
[5] Macey, R.L. and Farmer, R.E.L. (1970) Biochim. Biophys. Acta 211, 104–106.
[6] LeFevre, P.G. (1961) Pharmacol. Rev. 13, 39–70.
[7] Jordan, P. (1987) Biophys. J. 51, 297–311.
[8] Antonenko, Y.N. and Bulychev, A.A. (1991) Biochim. Biophys. Acta 1070, 474–480.
[9] Bechinger, B. and Seelig, J. (1991) Biochemistry 30, 3923–3929.
[10] Gawrisch, K., Ruston, D., Zimmerberg, J., Parsegian, V.A., Rand, R.P. and Fuller, N. (1992) Biophys. J. 61, 1213–1223.
[11] Reyes, J., Greco, F., Motais, R. and Latorre, R. (1983) J. Membr. Biol. 72, 93–103.
[12] Verkman, A.S. and Solomon, A.K. (1982) J. Gen. Physiol. 80, 557–581.
[13] Sokolov, V.S., Cherny, V.V., Simonova M.V. and Markin, V.S. (1990) Bioelectroch. Bioenerg. 23, 27–44.
[14] Markin, V.S., Portnov, V.I., Simonova, M.V., Sokolov, V.S. and Cherny, V.V. (1987) Biol. Membr. 4, 502–523 (in Russian).
[15] Horn, L.W. (1993) Biophys. J. 64, 281–289.
[16] Wang, J., Wehner, G., Benz, R. and Zimmermann, U. (1993) Biophys. J. 64, 1657–1667.
[17] Verkman, A.S. and Solomon, A.K. (1980) J. Gen. Physiol. 75, 673–692.
[18] Verkman, A.S. (1980) Biochim. Biophys. Acta 599, 370–379.
[19] Gross, E., Bedlack, R.S. and Loew, L.M. (1994) Biophys. J. 67, 208–216.
[20] Awiszus, R. and Stark, G. (1988) Eur. Biophys. J. 15, 321–328.
[21] Jennings, M.L. and Solomon, A.K. (1976) J. Gen. Physiol. 67, 381–397.
[22] Gutknecht, J. and Tosteson, D.C. (1973) Science 182, 1258–1261
[23] Antonenko, Y.N., Denisov, G.A. and Pohl, P. (1993) Biophys. J. 64, 1701–1710.
[24] De Levie, R., Rangarajan, S.K. and Seelig, P.F. (1979) Biophys. J. 25, 295–300.
[25] Mueller, P., Rudin, D.O., Tien, H.T. and Wescott, W.C. (1963) J. Phys. Chem. 67, 534–535.
[26] Alvarez, O. and Latorre, R. (1978) Biophys. J. 21, 1–17.
[27] Pohl, P., Antonenko, Y.N. and Rosenfeld, E. (1993) Biochim. Biophys. Acta 1152, 155–160.
[28] Walter, A., Hastings, D. and Gutknecht, J. (1982) J. Gen. Physiol. 79, 917–933.
[29] Pohl, P., Rosenfeld, E. and Millner, R. (1993) Biochim. Biophys. Acta 1145, 279–283.
[30] Antonenko, Y.N. and Yaguzhinsky, L.S. (1982) J. Bioenerg. Biomembr. 14, 457–465.
[31] Walter, A. and Gutknecht, J. (1982) J. Membr. Biol. 77, 255–264.
[32] Walter, A. and Gutknecht, J. (1986) J. Membr. Biol. 90, 207–217.
[33] Flewelling, R.F. and Hubbell, W.L. (1986) Biophys. J. 49, 541–552.
[34] Sokolov, V.S., Cherny, V.V. and Markin, V.S. (1984) Biofizika 29, 424–429 (in Russian).
[35] Cevc, G. (1990) Biochim. Biophys. Acta 1031, 311–382.